APPLICATION OF BERLIN'S THEOREM TO BOND-LENGTH CHANGES IN ISOLATED MOLECULES AND RED- AND BLUE-SHIFTING H-BONDED CLUSTERS

Weizhou WANG[1] and Pavel HOBZA[2],*

Institute of Organic Chemistry and Biochemistry, Academy of Sciences of the Czech Republic, v.v.i. and Center for Biomolecules and Complex Molecular Systems, Flemingovo nám. 2, 166 10 Prague 6, Czech Republic; e-mail: [1] weizhou.wang@marge.uochb.cas.cz, [2] pavel.hobza@uochb.cas.cz

Dedicated to Professor Rudolf Zahradník on the occasion of his 80th birthday.

The origin of the bond-length change in molecule or molecular cluster has been investigated at the MP2/aug-cc-pVDZ level of theory using the electrostatic potential or the electron density difference analysis method. Our results have clearly shown that the bond-length change of a chemical bond is determined mainly by the balance of the electrostatic forces exerted by electrons on the two nuclei. The factors that affect the balance of the electrostatic forces include four parts: (i) The abstraction of the electron density from Berlin's binding region between the two nuclei. (ii) The accumulation of the electron density in Berlin's antibinding regions. (iii) The accumulation of the electron density in Berlin's binding region between the two nuclei. (iv) The abstraction of the electron density from Berlin's antibinding regions. Using the change of the electron density around the two nuclei of a chemical bond, we have succeeded in explaining two important chemical phenomena: (i) breakdown of bond length–bond strength correlation; (ii) the bond-length change in the hydrogen bond.
Keywords: Berlin's theorem; H-bonding; Blue-shifting H-bonding.

Chemistry is a science of change in which the structural change of compounds plays a pivotal role because the structure and bonding of a compound determine its chemical and physical properties. Then, an important question is: What is the origin of the change of the structure? The search for the answer has a long history. But even in recent years, there are still debates going on about whether or not the wave function or the electron density is the more fundamental for understanding chemical bonding and molecular geometry[1–4]. Despite the controversy, it is still useful to use the energy or the electron density to analyze and solve chemical problems. In

the present study, we mainly focus on the correlation between electron density distribution and molecular geometries.

To study the origin of the bond-length change is the first step for the understanding of the structural change of the whole molecule. Let us add here that the bond-length change itself is a very important topic in chemistry. For example, the substitution of one or more atoms in a molecule always results in the bond-length change of the unsubstituted chemical bond, and, for the molecular cluster, the change of the stretching frequency upon complexation is usually accompanied by the bond-length change of the corresponding chemical bond. At the same time, it is well known that the bond-length change is related to the nature of the chemical bond. In 1951, Berlin defined the binding and antibinding regions in a diatomic molecule according to the forces acting on the two nuclei (Fig. 1a)[5]. He pointed out that the electron density in a binding region tends to shorten the bond, whereas in an antibinding region it tends to elongate the bond. Later, Spackman and Maslen extended Berlin's idea and proposed that not only electron density accumulation in binding regions, but also electron density abstraction from antibinding regions may result in the bond contraction, and, similarly, both electron density depletion in binding regions and electron density accumulation in antibinding regions may cause the bond to elongate[6]. However, for the polyatomic molecules and molecular clusters, it is difficult to accurately define Berlin's binding regions and Berlin's antibinding regions[7,8]. Since only the electron density near the two nuclei is important for the change of the bond length, we may consider the polyatomic molecule or the molecular cluster approximately as a pseudo-diatomic species: The region between the two nuclei of the chemical bond can be identified with Berlin's binding region and the regions outside the
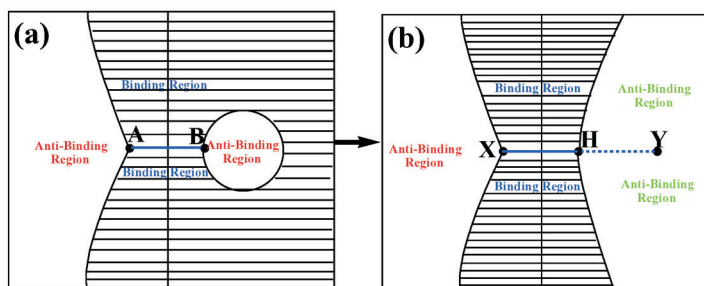

Fig. 1

Binding and antibinding regions in a heteronuclear diatomic molecule AB (a) and a hydrogen-bonded complex with the type of X–H···Y (b)

two nuclei can be identified with Berlin's antibinding region[9]. Figure 1 shows the binding and antibinding regions of a X–H···Y hydrogen-bonded complex. The antibinding region marked by green colour in Fig. 1b is different from others (marked in red) because the electrostatic attractive interaction between positive H and negative Y always yields the X–H bond elongation. Using this approximation the Berlin's theorem explaining the origin of the bond-length change can be applied for both molecules and molecular clusters.

The general rule for the bond length–bond strength relationship is following – longer bond is weaker bond and shorter bond is stronger bond. However, an unusual relationship between the bond length and the bond strength has been found in many studies[10–12]. Kaupp and coworkers explained the breakdown of bond length–bond strength correlation on the basis of hybridization defects[12]. Here, we reinvestigate this issue and explain it on the basis of the change of the electron density. Another important issue related to the bond length is the bond-length change of the hydrogen bond. Generally, the X–H···Y hydrogen bond is characterized by an elongation of the X–H bond and a decrease of its stretching frequency[13]. But in recent years, a number of theoretical and experimental studies have demonstrated that there also exists a new type of hydrogen bond – the blue-shifting hydrogen bond, in which the X–H bond shortening and associated blue shift are observed[14–22]. In the present paper, we will investigate the origin of the X–H bond-length change employing the Berlin's theorem. It must be pointed out here that Berlin's theorem can also be applied to solving similar problems, such as the origin of the bond-length change in the lithium bond, the origin of the bond-length change in the halogen bond, etc.[23–25]

METHODS

Geometry optimizations of the molecules and the molecular clusters were performed using the Gaussian03 suite of programs[26]. All calculations were done using the second-order Møller–Plesset perturbation theory (MP2) in conjunction with the Dunning augmented correlation-consistent basis set aug-cc-pVDZ [27].

The electrostatic potential for the molecules HOF and FOF has been carried out using the MP2-optimized structure and the MP2 electron density. For the molecular clusters, a number of different proton donor molecules, including sp^3-, sp^2-, and sp-hybridized carbons, paired with benzene were considered. MP2 electron densities and their shifts were displayed using the

GaussView program[28]; values for the isosurfaces are denoted in the figure captions. The natural bond orbital (NBO) charge[29] was calculated at the HF/aug-cc-pVDZ//MP2/aug-cc-pVDZ level of theory using the built-in subroutine of the Gaussian03 program.

RESULTS AND DISCUSSION

Isolated Molecule

There are many cases in which shorter bonds have been found to have smaller bond energies[10–12]. In this paper, we selected O–F bonds in the molecules HOF and FOF to study the origin of breakdown of the bond length–bond strength correlation. Since the electrostatic potential is very directly and rigorously related to the electron density, we can use the change of the electrostatic potential to describe the change of the electron density. The positive electrostatic potential regions indicate a deficiency of electron density, while the negative potential regions indicate areas with an excess of electron density. An increase of the electrostatic potential value means a decrease of the electron density, and vice versa. Note that the electrostatic potential map is convenient to see the small changes in the electron density. Figure 2 shows the electrostatic potential maps of HOF and FOF on
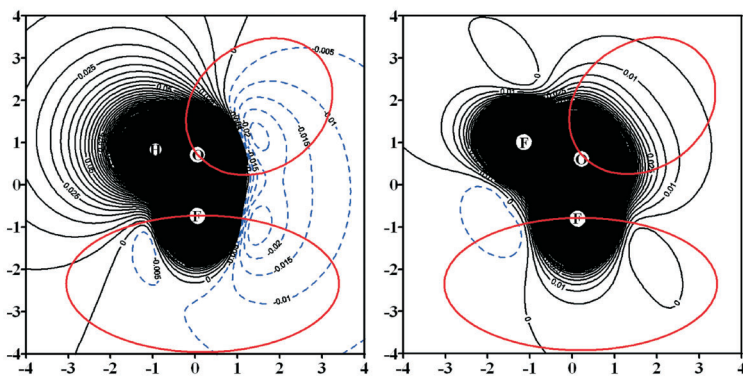

Fig. 2

Electrostatic potential maps of HOF and FOF on the molecular plane. The black lines represent the positive part of the electrostatic potential, the blue ones represent the negative part of the electrostatic potential. The contour interval is 0.005 a.u. The unit of the axes is Å. The regions inside the red ellipses can be approximately identified with Berlin's antibinding region. For the definitions of Berlin's binding and antibinding regions of triatomic molecules, see ref.[7] for details

their respective molecular plane. As mentioned above, we only focus on Berlin's binding region that is between O and F and Berlin's antibinding regions that are at the rears of O and F away from the O–F bond including the lone-pair regions (see Fig. 2). It can be clearly seen from Fig. 2 that the electron density decreases in the region between O and F after the replacement of a hydrogen by a fluorine (blue lines at the right of vertical O–F bond are upon replacement of H by F changed into black ones; this change indicates electron density decrease). According to Berlin's theorem, the decrease of electron density in the binding region results in the elongation of the O–F bond. In the O–F Berlin's antibinding regions the electron density also decreases after the fluorine substitution (blue lines in antibinding regions indicated by red ellipses are upon F substitution changed into black lines) and this decrease is more significant than that in the binding region between O and F. This is mainly apparent at the lone-pair regions of O and F where the negative electrostatic potential (little blue circle regions visible in case of HOF) disappears almost completely after the fluorine substitution. The electron density decrease in Berlin's antibinding regions leads to decrease of the electrostatic Hellmann–Feynman force acting on the two nuclei and, consequently, the contraction of the O–F bond. The shortening effect dominates and the O–F bond is finally contracted. According the MP2/aug-cc-pVDZ calculations, the O–F bond length in the HOF and FOF molecules equals to 1.4461 and 1.4221 Å, respectively, which is in agreement with the available experimental value of 1.442 Å for HOF and 1.409 Å for FOF [11]. On the other hand, the decrease of the electron density in the binding region (see above) weakens the O–F bond. The computational and experimental values of force constants and dissociation energies for the O–F bonds in HOF and FOF did show a marked decrease with increasing fluorination[11]. Now, we can see that the reason for the unusual correlation between bond length and bond strength is successfully explained by applying the electron-density changes in the Berlin's binding and antibinding regions.

Red- and Blue-Shifting H-Bonded Clusters

When two or more systems interact their bond lengths are usually changed. One of the most important examples is the change of the X–H bond length upon formation of the X–H⋯Y hydrogen bond. The origin of the X–H bond length change has been explored by many studies[14–22], but none of the explanations are general and some conclusions and results even contradict each other[14–22].

In the present paper, we investigate the origin of the bond-length change upon molecular cluster formation and we selected the following complexes: $CH_4\cdots C_6H_6$, $C_6H_6\cdots C_6H_6$ and $HCCH\cdots C_6H_6$. Besides the C–H bond directly involved in the hydrogen bond, we also considered the other C–H bonds in the proton donors CH_4, C_6H_6 and HCCH which do not directly participate in the H-bonding.

The left side in Fig. 3 shows the dependence of the C–H bond-length change on the distance between H_a and Y. $C–H_b$ and $C_b–H_b$ distances in $CH_4\cdots C_6H_6$ and in $C_6H_6\cdots C_6H_6$ complexes both increase continuously with the decrease of the $H_a\cdots Y$ distance. The C–H bonds involved in the hydrogen bond in both complexes first decrease and then increase with the decrease of the $H_a\cdots Y$ distance. For the complex $HCCH\cdots C_6H_6$, the change of the C–H bonds is more complicated: the $C_a–H_a$ bond length first slightly increases, then decreases, and finally increases again with the decrease of the $H_a\cdots Y$ distance. The $C_b–H_b$ bonds are all contracted in the range of 1.8–6.5 Å of the $H_a\cdots Y$ distance.

Investigating the C and H NBO charges in Table I, we find that the H_b charges in all three complexes are decreased with the decrease of the $H_a\cdots Y$ distance. This indicates a net shift of charge toward the $C_b(C)–H_b$ end. Table I further shows that the H_a charges first increase and then decrease with the decrease of the $H_a\cdots Y$ distance. Charges on C atoms involved in the C–H$\cdots\pi$ hydrogen bond are all increased with the decrease of the $H_a\cdots Y$ distance while the charges on C_b atoms in $C_6H_6\cdots C_6H_6$ and $HCCH\cdots C_6H_6$ complexes decreased with the decrease of the $H_a\cdots Y$ distance. However, in the case of benzene$\cdots$HF dimer the opposite was found; the charge on the F atom decreased with the decrease of the H$\cdots$Y distance[30]. We can thus conclude that there is no correlation between the charge change and the bond-length change.

Let us further investigate the electron density difference maps. As shown in the right side of the Fig. 3, the electron densities in the remote part of the proton donors increased with the decrease of the $H_a\cdots Y$ distance (compare electron densities of the red-shifting H-bonded complex and the corresponding blue-shifting H-bonded complex). Simultaneously, these electron densities also increased upon the complex formation (see electron density for each complex). The electron density increase in the remote part of the proton donors of all complexes is more pronounced at shorter $H_a\cdots Y$ distances where all complexes exhibited a red shift of the C–H stretch frequency. The same is true for the increase or decrease of the electron density in other regions. The explanation of the origin of the bond-length change from the electron density difference maps is thus relatively simple for the
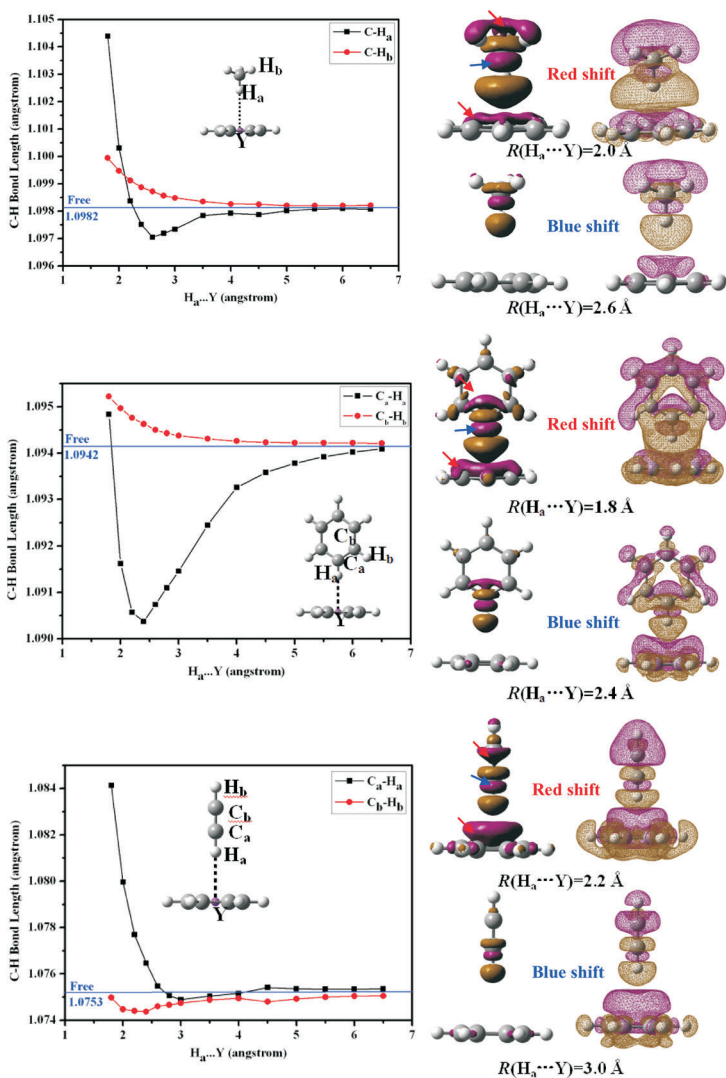
FIG. 3
Change of the C–H bond length with the distance between H_a and Y and selected electron density difference maps for the complexes $CH_4\cdots C_6H_6$, $C_6H_6\cdots C_6H_6$ and $HCCH\cdots C_6H_6$. In the electron density difference maps, red regions denote gain and yellow regions represent loss. Contour illustrated in solid format corresponds to change by 0.0004 a.u. and the contour interval is 0.0001 a.u. for those illustrated in mesh format. The regions which the red arrows point to can be approximately defined as the Berlin's antibinding regions and the regions which the blue arrows point to can be approximately defined as the Berlin's binding regions

C–H bonds not involved in the hydrogen bond. The electron density between C and H_b and C_b and H_b in $CH_4{\cdots}C_6H_6$ and $C_6H_6{\cdots}C_6H_6$ complexes both decreased upon complex formation while electron densities at the rears of C and H_b, and C_b and H_b in $CH_4{\cdots}C_6H_6$ and $C_6H_6{\cdots}C_6H_6$ complexes both increased upon complex formation. According to Berlin's theorem, this will lead to elongation of $C–H_b$ and $C_b–H_b$ bonds. The situation is more complicated for the $C_b–H_b$ in $HCCH{\cdots}C_6H_6$ complex. The electron density between C_b and H_b decreased and the electron density at the rear of H_b increased. However, the electron density at the rear of C_b, i.e. the electron density around C_a also decreased. The former effect indicated bond elongation while the latter effect the bond contraction. Since the latter effects are dominant the $C_b–H_b$ bond was finally contracted.

The explanation for $C_a(C)–H_a$ bond-length change is, however, more complex. Let us first define the Berlin's binding and antibinding regions. The blue arrows in Fig. 3 define the former regions and the red arrows indi-

TABLE I
Change of the NBO charge (in e) on atoms C or H in the proton donors of the complexes $CH_4{\cdots}C_6H_6$, $C_6H_6{\cdots}C_6H_6$ and $HCCH{\cdots}C_6H_6$ with the distance between H_a and Y

$H_a{\cdots}Y$	$CH_4{\cdots}C_6H_6$			$C_6H_6{\cdots}C_6H_6$				$HCCH{\cdots}C_6H_6$			
	$q(H_a)$	$q(C)$	$q(H_b)$	$q(H_a)$	$q(C_a)$	$q(C_b)$	$q(H_b)$	$q(H_a)$	$q(C_a)$	$q(C_b)$	$q(H_b)$
1.8	0.189	–0.760	0.185	0.208	–0.190	–0.225	0.213	0.222	–0.195	–0.288	0.236
2.0	0.192	–0.764	0.187	0.210	–0.193	–0.223	0.214	0.226	–0.200	–0.280	0.237
2.2	0.195	–0.769	0.188	0.213	–0.198	–0.222	0.215	0.231	–0.206	–0.274	0.237
2.4	0.198	–0.773	0.190	0.217	–0.203	–0.221	0.216	0.236	–0.212	–0.269	0.237
2.6	0.200	–0.776	0.191	0.221	–0.207	–0.221	0.217	0.239	–0.218	–0.265	0.238
2.8	0.202	–0.779	0.191	0.224	–0.211	–0.220	0.217	0.242	–0.223	–0.262	0.238
3.0	0.203	–0.781	0.192	0.226	–0.213	–0.220	0.217	0.244	–0.227	–0.259	0.238
3.5	0.203	–0.784	0.193	0.227	–0.217	–0.220	0.218	0.246	–0.232	–0.254	0.239
4.0	0.202	–0.784	0.194	0.225	–0.217	–0.220	0.219	0.246	–0.236	–0.251	0.239
4.5	0.200	–0.784	0.194	0.223	–0.217	–0.220	0.219	0.244	–0.237	–0.248	0.240
5.0	0.199	–0.784	0.195	0.222	–0.218	–0.219	0.219	0.244	–0.238	–0.246	0.240
5.5	0.198	–0.784	0.195	0.221	–0.218	–0.219	0.219	0.243	–0.238	–0.245	0.240
6.0	0.198	–0.783	0.195	0.221	–0.218	–0.219	0.219	0.243	–0.239	–0.244	0.240
6.5	0.197	–0.783	0.195	0.221	–0.219	–0.219	0.219	0.242	–0.239	–0.244	0.241
Free	0.196	–0.783	0.196	0.219	–0.219	–0.219	0.219	0.241	–0.241	–0.241	0.241

cate the latter regions. Investigating the electron density difference maps with contour interval 0.0001 a.u. in Fig. 3 (mesh format), we found that the electron densities in Berlin's binding and antibinding regions all increased for shorter as well as for longer H_a–Y distances (i.e. for both red-shifting and blue-shifting hydrogen bonds). Obviously, there exists a balance that determines the net bond-length change. Investigating the electron density difference maps with contour interval 0.0004 a.u. (Fig. 3, the solid format) we found for the red-shifting hydrogen bond that the electron density accumulation in the Berlin's antibinding regions plays a dominant role and causes the $C_a(C)$–H_a bond elongation. For the blue-shifting hydrogen bond, the increase of the electron density at the back of $C_a(C)$ and above the plane of the benzene ring is, however, not noticeable. Therefore, the electron density accumulation between $C_a(C)$ and H_a dominates and, consequently, the $C_a(C)$–H_a bond shortens. In a recent paper, Jemmis and Joseph provided a uniform explanation for the red, blue, or no shift in hydrogen bonds[22]. They claimed that the net gain of electron density at the X–H region encourages an X–H bond contraction, and the electrostatic attractive interaction between the positive H and the negative Y causes an X–H elongation. We extend this explanation by considering the electron density change in the region at the rear of X away from X–H bond. The present explanation works also for the X–H bond not involved in the hydrogen bond.

We conclude that the electron density increase at the rears of the atoms X and H away from the X–H bond is one of players determining the red-shifting character. This increase is not obvious for the blue-shifting hydrogen bond.

CONCLUSIONS

The region near the two nuclei of the chemical bond is approximately divided into three parts. The first part localized between the two nuclei is defined as Berlin's binding region. The other two parts localized at the rear of the two nuclei away from the chemical bond, are defined as Berlin's antibinding regions. The elongation of a chemical bond is caused by the abstraction of the electron density from Berlin's binding region between the two nuclei or by the accumulation of the electron density in Berlin's antibinding regions; the contraction of a chemical bond is accompanied by the accumulation of the electron density in between the two nuclei or by the abstraction of the electron density from Berlin's antibinding regions. The net bond-length change is mainly determined by the balance of the four factors, or we can say by the balance of the electrostatic forces exerted by

electrons on the two nuclei. Our results have clearly shown that it is the net change of the electron density that determines the origin of the bond-length change of separated molecule upon fluorine substitution and the origin of the bond-length change in the hydrogen-bonded complex upon complexation. The X–H bond-length change in the hydrogen bond is determined by the electron density changes in three regions, that is, the region between X and H, the region at the rear of X and the region between H and Y. The explanation for the origin of the X–H bond-length change will be incomplete without considering any one of them.

REFERENCES

1. Frenking G.: *Angew. Chem. Int. Ed.* **2003**, *42*, 143.
2. Gillespie R. J., Popelier P. L. A.: *Angew. Chem. Int. Ed.* **2003**, *42*, 3331.
3. Bader R. F. W.: *Chem. Eur. J.* **2006**, *12*, 7769.
4. Frenking G.: *Chem. Eur. J.* **2006**, *12*, 7773.
5. Berlin T.: *J. Chem. Phys.* **1951**, *19*, 208.
6. Spackman M. A., Maslen E. N.: *Acta Crystallogr., Sect. A: Fundam. Crystallogr.* **1985**, *41*, 347.
7. Bader R. F. W.: *J. Am. Chem. Soc.* **1964**, *86*, 5070.
8. Koga T., Nakatsuji H., Yonezawa T.: *J. Am. Chem. Soc.* **1978**, *100*, 7522.
9. Fajans K.: *Chem. Eng. News* **1949**, *27*, 900.
10. Christen D., Gupta O. D., Kadel J., Kirchmeier R. L., Mack H. G., Oberhammer H., Shreeve J. M.: *J. Am. Chem. Soc.* **1991**, *113*, 9131.
11. Politzer P., Habibollahzadeh D.: *J. Chem. Phys.* **1993**, *98*, 7659.
12. Kaupp M., Metz B., Stoll H.: *Angew. Chem. Int. Ed.* **2000**, *39*, 4607.
13. Scheiner S.: *Hydrogen Bonding*. Oxford University Press, New York 1997.
14. Hobza P., Špirko V., Selzle H. L., Schlag E. W.: *J. Phys. Chem. A* **1998**, *102*, 2501.
15. Hobza P., Havlas Z.: *Chem. Rev.* **2000**, *100*, 4253.
16. Gu Y., Kar T., Scheiner S.: *J. Am. Chem. Soc.* **1999**, *121*, 9411.
17. Scheiner S., Kar T.: *J. Phys. Chem. A* **2002**, *106*, 1784.
18. Hermansson K.: *J. Phys. Chem. A* **2002**, *106*, 4695.
19. Li X., Liu L., Schlegel H. B.: *J. Am. Chem. Soc.* **2002**, *124*, 9639.
20. Alabugin I. V., Manoharan M., Peabody S., Weinhold F.: *J. Am. Chem. Soc.* **2003**, *125*, 5973.
21. McDowell S. A. C., Buckingham A. D.: *J. Am. Chem. Soc.* **2005**, *127*, 15515.
22. Joseph J., Jemmis E. D.: *J. Am. Chem. Soc.* **2007**, *129*, 4620.
23. Feng Y., Liu L., Wang J. T., Li X. S., Guo Q. X.: *Chem. Commun.* **2004**, *1*, 88.
24. Wang W. Z., Wong N. B., Zheng W. X., Tian A. M.: *J. Phys. Chem. A* **2004**, *108*, 1799.
25. Wang W. Z., Hobza P.: *J. Phys. Chem. A* **2008**, *112*, 4114.

26. Frisch M. J., Trucks G. W., Schlegel H. B., Scuseria G. E., Robb M. A., Cheeseman J. R., Montgomery J. A., Jr., Vreven T., Kudin K. N., Burant J. C., Millam J. M., Iyengar S. S., Tomasi J., Barone V., Mennucci B., Cossi M., Scalmani G., Rega N., Petersson G. A., Nakatsuji H., Hada M., Ehara M., Toyota K., Fukuda R., Hasegawa J., Ishida M., Nakajima T., Honda Y., Kitao O., Nakai H., Klene M., Li X., Knox J. E., Hratchian H. P., Cross J. B., Adamo C., Jaramillo J., Gomperts R., Stratmann R. E., Yazyev O., Austin A. J., Cammi R., Pomelli C., Ochterski J. W., Ayala P. Y., Morokuma K., Voth G. A., Salvador P., Dannenberg J. J., Zakrzewski V. G., Dapprich S., Daniels A. D., Strain M. C., Farkas O., Malick D. K., Rabuck A. D., Raghavachari K., Foresman J. B., Ortiz J. V., Cui Q., Baboul A. G., Clifford S., Cioslowski J., Stefanov B. B., Liu G., Liashenko A., Piskorz P., Komaromi I., Martin R. L., Fox D. J., Keith T., Al-Laham M. A., Peng C. Y., Nanayakkara A., Challacombe M., Gill P. M. W., Johnson B., Chen W., Wong M. W., Gonzalez C., Pople J. A.: *Gaussian03*, Revision C.02. Gaussian Inc., Wallingford (CT) 2004.
27. Dunning T. H.: *J. Chem. Phys.* **1989**, *90*, 1007.
28. Dennington R., Jr., Keith T., Millam J., Eppinnett K., Hovell W. L., Gilliland R.: *GaussView*. Semichem Inc., Shawnee Mission (KS) 2003.
29. Reed A. E., Curtiss L. A., Weinhold F.: *Chem. Rev.* **1988**, *88*, 899.
30. Wang S.-C., Sahu P. K., Lee S.-L.: *Chem. Phys. Lett.* **2005**, *406*, 143.